

## Supplemental Materials for

### Structural and magnetic phase diagram of CrAs and its relationship with pressure induced superconductivity

Yao Shen,<sup>1</sup> Qisi Wang,<sup>1</sup> Yiqing Hao,<sup>1</sup> Bingying Pan,<sup>1</sup> Yu Feng,<sup>1</sup> Q. Huang,<sup>2</sup> L. W. Harriger,<sup>2</sup> J. B. Leao,<sup>2</sup> Y. Zhao,<sup>2,3</sup> R. M. Chisnell,<sup>2</sup> J. W. Lynn,<sup>2</sup> Huibo Cao,<sup>4</sup> Jiangping Hu,<sup>5,6</sup> and Jun Zhao<sup>1,7,\*</sup>

<sup>1</sup> State Key Laboratory of Surface Physics and Department of Physics, Fudan University, Shanghai 200433, China

<sup>2</sup> NIST Center for Neutron Research, National Institute of Standards and Technology, Gaithersburg, Maryland 20899, USA

<sup>3</sup> Department of Materials Science and Engineering, University of Maryland, College Park, Maryland 20742, USA

<sup>4</sup> Neutron Scattering Science Division, Oak Ridge National Laboratory, Oak Ridge, Tennessee 37831-6393, USA

<sup>5</sup> Institute of Physics, Chinese Academy of Sciences, Beijing 100190, China

<sup>6</sup> Department of Physics, Purdue University, West Lafayette, Indiana 47907, USA

<sup>7</sup> Collaborative Innovation Center of Advanced Microstructures, Fudan University, Shanghai 200433, China

#### I. Sample characterizations, neutron scattering experiment configurations, and refined structure parameters

The susceptibility of our sample displays a clear anomaly near 270 K (Figure S1), indicating a magnetic phase transition. Our neutron scattering measurements were carried out on the BT-1 powder diffractometer, SPINS cold triple-axis spectrometer, and BT-7 thermal triple axis spectrometer at the NIST Center for Neutron Research. The neutron wavelengths employed were 1.5389 or 2.0785 Å using the Ge(311) monochromator at BT-1, 4.0449 Å using PG (002) monochromator at SPINS, and 2.36 Å using PG (002) monochromator at BT-7. The neutron-diffraction data Rietveld refinements are based on the program FULLPROF [1]. The refined structural parameters at representative temperature and pressure are provided in Table SI. For both susceptibility and neutron scattering measurements, we were not able to cool the sample below 1.5 K, so only the normal state structural and magnetic properties were studied.

#### II. Details about the pressure effect measurements

For the pressure effect measurements, the polycrystalline sample was loaded into an aluminium alloy or steel pressure cell, which was connected to an external piston-driven pressure intensifier via a heated capillary line, and pressurized using helium as a pressure medium. All pressure changes were executed while maintaining the pressure vessels above the PxT line of helium. For the measurements below the PxT line of helium, hydrostatic conditions were maintained by employing a “BURP” process (a careful

**Table S I:** Refined structural parameters of CrAs under ambient and applied pressure. Space group:  $Pnma$ . Atomic positions: Cr:  $4c(x, 1/4, z)$ ; As:  $4c(x, 1/4, z)$ .

Atom		0 GPa, 4 K	0 GPa, 290 K	0.4 GPa, 4 K	0.4 GPa, 210 K	0.6 GPa, 50 K	0.6 GPa, 170 K
	$a(\text{\AA})$	5.60499(5)	5.65101(8)	5.5882(1)	5.6448(1)	5.5700(1)	5.6411(2)
	$b(\text{\AA})$	3.58827(3)	3.46398(5)	3.57937(7)	3.40203(8)	3.57003(9)	3.38452(9)
	$c(\text{\AA})$	6.13519(5)	6.20804(8)	6.1253(1)	6.2106(1)	6.1176(1)	6.2082(1)
Cr	$x$	0.0070(2)	0.0060(3)	0.0093(5)	0.0091(5)	0.0086(7)	0.0081(7)
	$z$	0.2049(2)	0.2019(3)	0.2029(4)	0.1994(5)	0.2015(5)	0.1992(6)
	$B(\text{\AA}^2)$	0.15(2)	0.74(5)	0.14(5)	0.32(6)	0.08(8)	0.27(8)
As	$x$	0.2045(1)	0.2016(2)	0.2026(2)	0.1985(3)	0.1990(3)	0.1979(4)
	$z$	0.5836(1)	0.5766(2)	0.5837(3)	0.5738(3)	0.5822(4)	0.5726(4)
	$B(\text{\AA}^2)$	0.03(1)	0.58(3)	0.44(3)	0.24(2)	0.37(6)	0.17(7)
	$R_p(\%)$	4.82	6.63	4.73	4.81	5.86	5.40
	$wR_p(\%)$	5.87	8.21	5.95	5.91	7.05	6.69
	$\chi^2$	1.55	1.40	2.00	1.25	1.10	0.97

pressurization procedure in order to ensure pressure homogeneity within the pressure cells).

### III. Re-analyse of the diffraction data in ref. 2

In ref. 2 (ref. 16 of the main text of the paper), neutron diffraction measurements were performed at  $P \leq 0.65$  GPa using a fluorocarbon-based fluid pressure medium in a clamp pressure cell, and the spin reorientation was not found. However, we believe that this discrepancy is because of significant pressure inhomogeneity in the pressure cell in ref. 2 and inappropriate analysis of the data. Fig. S2 shows the pressure dependence of neutron diffraction patterns reported in ref. 2. We notice that the Bragg peaks under pressure are much broader than at ambient pressure. Close inspection of the data reveals that there are at least two sets of Bragg peaks (Miller index in red indicates phase  $a$  and black indicates phase  $b$ ), in contrast to our data that only one set of *sharp* Bragg peaks is observed at similar pressure range (Figs. 1c-1e). The presence of two sets of Bragg peaks suggests significant pressure inhomogeneity in the pressure cell. This makes it difficult to determine the magnetic structure under pressure, since the part of the sample that experiences lower pressure tends to give stronger magnetic signals. Moreover, neglecting the phase separation caused inaccurate estimation of lattice parameters and wavevectors. Consequently, the Rietveld refinement reported in ref. 2 failed to identify the  $(110\pm)$  magnetic Bragg peak (marked by blue arrows in

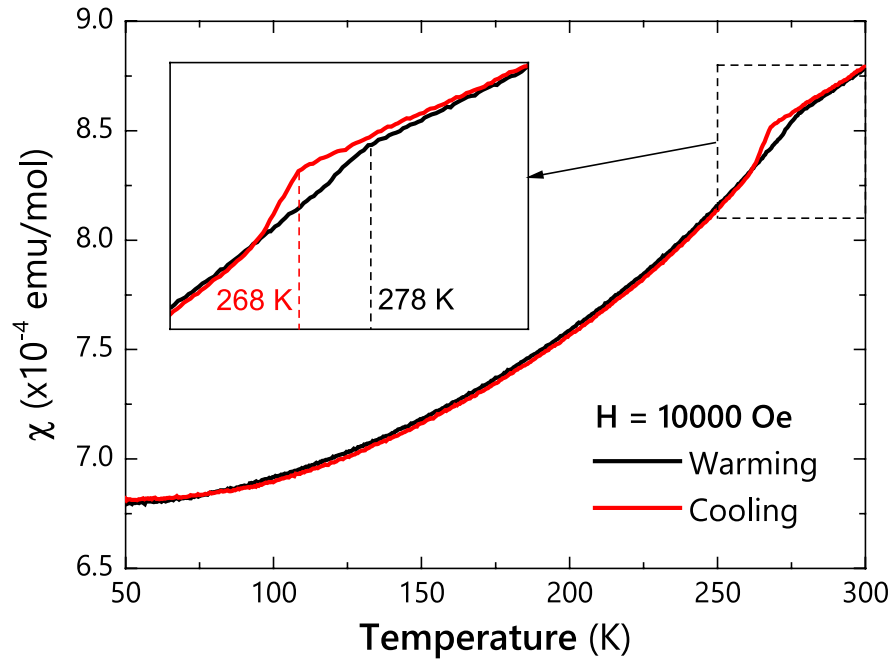


**Figure S 1:** Temperature dependence of the magnetic susceptibility of polycrystalline CrAs. Magnetization measurements were performed in a Quantum Design superconducting quantum interference device (SQUID) magnetometer. The temperature dependence of the magnetic susceptibility displays a clear anomaly near 270 K. The inset shows the thermal hysteresis near 270 K.

Fig. S2) under pressure. Therefore, it is clear that the data and analysis of ref. 2 were not established well enough to identify the spin reorientation of CrAs under pressure. Nevertheless, we notice that the  $(110\pm)$  magnetic peak seems to be vanishing more slowly than other magnetic peaks with increasing pressure (Fig. S2). This is actually an indication of the spin reorientation, because  $(110\pm)$  peak is indeed relatively strong in the spin reorientated high pressure phase (See Figs. 1c-1e).

---

\* Electronic address: zhaoj@fudan.edu.cn

[1] J. Rodriguez-Carvajal *Physica B* **192**, 55 (1993)

[2] L. Keller, J. S. White, M. Frontzek, P. Babkevich, M. A. Susner, Z. C. Sims, A. S. Sefat, H. M. Rønnow and C. Rüegg, *Phys. Rev. B* **91**, 020409 (2015).

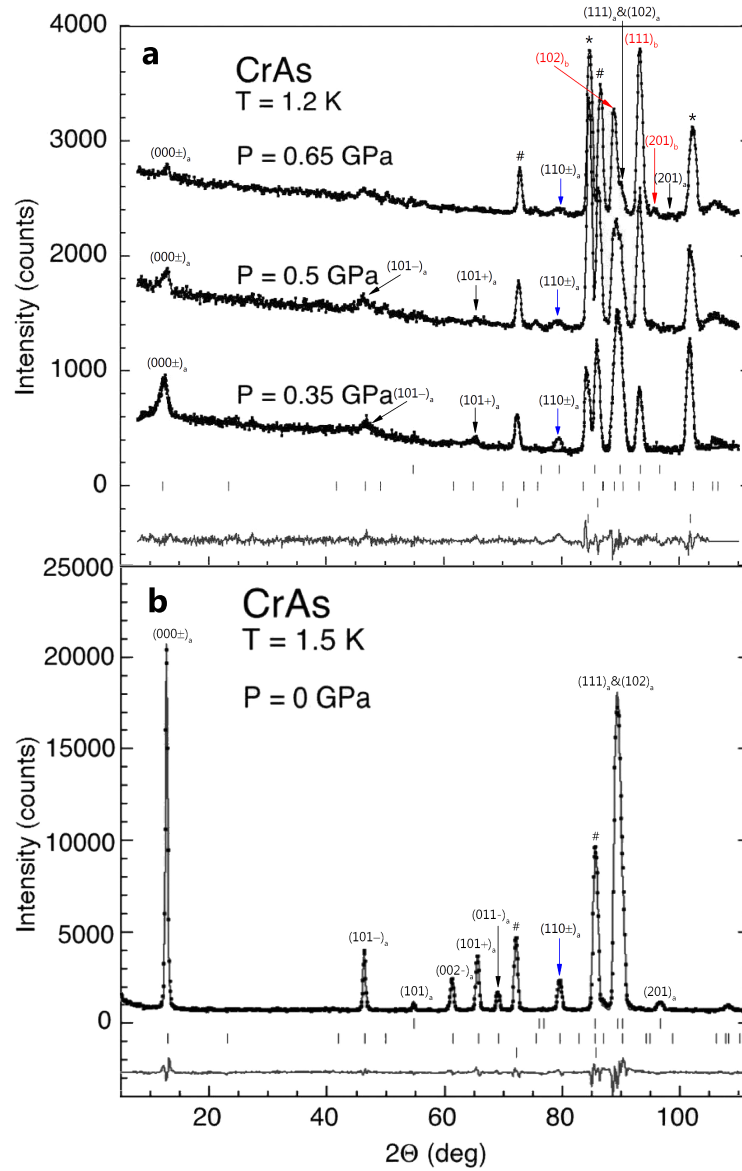


**Figure S 2:** Pressure dependence of neutron diffraction patterns adapted in ref. 2. The nuclear and magnetic Bragg peaks are re-indexed based on our analysis. Miller index in red indicates phase *a* and black indicates phase *b*. Hashtags and asterisks represent nuclear peaks of NaCl for pressure calibrant and Pb for sample capsule, respectively. Phases refined in the original graph are the crystal and magnetic structures of CrAs, crystal structures of NaCl and Pb, respectively. The original indices of CrAs phases are inaccurate as a consequence of neglecting the phase separation under pressure.